

Phase diagram for strongly correlated doped *trans*-polyacetylene chains

Luis Cruz

Room 6-222B, Department of Physics, Massachusetts Institute of Technology, Cambridge, Massachusetts 02139

Philip Phillips

Department of Physics, Loomis Laboratory, University of Illinois, Urbana, Illinois 61801-3080

(Received 10 September 1993)

We study here the stability of soliton and polaron excitations in a single strand of *trans*-polyacetylene as a function of the strength of the electron-electron correlations as well as the doping level. We proceed by first solving exactly the continuum version of the Su, Schrieffer, and Heeger Hamiltonian for the single-particle states that arise when electrons are added to a single polymer chain. The role of on-site (U), nearest-neighbor (V), and bond repulsion (W) Coulomb interactions are then obtained from a first-order perturbative calculation with the exact single-particle states. By minimizing the total energy, we are able to determine the relative stability of polaron and soliton configurations. We show that, at a fixed doping level, a polaron lattice is favored over a soliton configuration provided that U and V exceed critical values. However, as the doping level is increased, we show that the critical values of U and V at which a soliton lattice converts to a polaron lattice increase significantly beyond experimentally accepted estimates. W is also shown to favor solitons. We estimate that at a doping level corresponding to the insulator-metal transition (5%), $U=4$ eV and $V=0.4$ eV, a soliton lattice is 0.6 eV lower in energy than the corresponding polaron lattice. If we argue that the insulator-metal transition in polyacetylene results from the onset of a polaron lattice at 5%, then our work places restrictions on the magnitude of such effects as interchain coupling which have been proposed in the literature as a principal player in the metal transition in polyacetylene.

I. INTRODUCTION

Because the ground state of *trans*-polyacetylene is two-fold degenerate, polyacetylene is a Peierls band-gap insulator at half-filling. The degeneracy arises from the periodic arrangement of alternating double and single bonds (which constitute a commensurate charge-density wave) along the polymer backbone. Su, Schrieffer, and Heeger (SSH) have shown that the dimerization of the ground state of this polymer can be accounted for by a one-electron-phonon model with a periodic lattice distortion.¹ On physical grounds, one would suspect that because an on-site Hubbard U favors a uniform charge density, the tendency to dimerization at half-filling would desist if Hubbard-type interactions were turned on. A curious feature of *trans*-polyacetylene, however, is that electron correlations enhance dimerization at half-filling (Ref. 2 and references therein). This result, first established within the context of the extended Peierls-Hubbard models (see, for example, Ref. 3), certainly hinted that the phonon SSH model can only partially account for the ground state as well as conducting states of this polymer. Subsequent perturbative calculations,^{4,5} Monte Carlo,^{2,6} self-consistent numerical,⁷ and exact studies⁸ on finite systems have substantiated the finding that short-range electron correlations most likely dominate the dimerization process in the ground state.

Away from half-filling, there have been relatively few studies of the role of electron correlations in *trans*-polyacetylene. Such studies are of utmost importance if the precise mechanism of the insulator-metal transition in

polyacetylene is to be understood. The most dramatic experimental feature that a theory of the metal transition in polyacetylene must explain is the sudden onset of a Pauli susceptibility at a doping level of 5–6%.⁹ The lack of any discernible spin susceptibility below a doping level of 5–6% supports the view that charged solitonic rather than electron or holelike excitations form in the lightly doped form of the polymer. Such excitations populate the midgap states and are spinless. Kivelson and Heeger have suggested that the onset of a Pauli susceptibility in polyacetylene results from a transition from a soliton to a polaron lattice.¹⁰ Although this model would account for the Pauli susceptibility, it is inconsistent with the intense infrared active vibrational (IRAV) modes observed in the experiments of Kim and Heeger.¹¹ Kim and Heeger have observed that the intensity of the IRAV mode (a signature of solitonic excitations) increases as the doping level is increased. Nonetheless, it is believed that a transition to some kind of polaron lattice must obtain if itinerant spins are to form in the metallic state of *trans*-polyacetylene. Within the SSH one-electron-phonon model, only soliton excitations are stable, at all doping levels. Consequently, recent work on the metal transition in polyacetylene has focused on extensions of the SSH model that support polaron formation.^{12–14} For example, Mizes and Conwell¹⁴ have shown that interchain coupling as well as chain breaks stabilize polaron formation in *trans*-polyacetylene. These results were established for short chains containing at most one polaron. Attempts to explore the stability of polarons in single strands of polyacetylene have focused on perturbative studies of the

SSH model^{5,15} appended to an on-site Hubbard U .¹⁶ For values of U as large as 4.2 eV, it was found that solitons were favored over polarons regardless of the doping level. However, such studies treated the interactions at the Hartree level, and hence could not definitively answer the question as to the fate of polarons in single strands of *trans*-polyacetylene.

It is the purpose of this paper to address the issue of the role of short-range correlations along single strands of *trans*-polyacetylene as a function of doping. An on-site Hubbard U as well as a nearest-neighbor repulsion V will be used to describe the electron correlations. The continuum model of Takayama, Lin-Liu, and Maki (TLM) will be used to describe the SSH one-electron-phonon model.¹⁷ It will be shown that even in isolated chains a transition toward a polaron lattice can be achieved as the interaction strength increases. We find, moreover, that doping appears to favor a soliton state. In addition, we consider the role of a bond-charge Coulomb repulsion term W . It has been suggested⁴ that W stabilizes a polaron lattice. Exact numerical calculations of the ground state of short chains using this term at half-filling have demonstrated a transition from a dimerized to a ferromagnetic phase.¹⁸ We have performed calculations including this term in the total Hamiltonian, and show that contrary to accepted wisdom W favors a soliton lattice over a polaron lattice as a function of its strength and doping level in the chain.

A formalism will be presented that starts from the continuum TLM Hamiltonian,¹⁷ which is known to support both polarons and solitons as stable excitations.¹⁹ The doping dependence will be determined by calculating the energy levels of localized excitations that form in the midgap region when electrons are added to a single strand. The wave functions for these states will be obtained by using an inverse scattering theory for reflectionless bound states.²⁰ Because the resulting wave functions extrapolate smoothly from soliton to polaron excitations when the position of the bound-state energies in the gap is tuned, we will minimize the total energy with respect to these discrete energies in order to determine the stable configuration of solitons or polarons. The first-order perturbation theory for the full Hamiltonian will then be used to determine the role of correlations.^{21,22}

II. FORMALISM

The starting point of our analysis is the extended Peierls-Hubbard model

$$\mathcal{H} = \mathcal{H}_{\text{TLM}} + \mathcal{H}_U + \mathcal{H}_V + \mathcal{H}_W, \quad (1)$$

where \mathcal{H}_{TLM} is the continuum TLM Hamiltonian¹⁷

$$\begin{aligned} \mathcal{H}_{\text{TLM}} = & \frac{1}{2\pi\lambda v_F} \int dx \Delta(x)^2 \\ & + \int dx \Psi^\dagger [-iv_f \sigma_2 \partial_x + \Delta(x) \sigma_1] \Psi. \end{aligned} \quad (2)$$

In Eq. (2), $\Psi = (u, v)$ is the two-component spinor, v_f the Fermi velocity, $\Delta(x)$ the order parameter, and the σ_i 's are Pauli matrices. Parameter λ denotes the elastic energy coupling constant, and the convention $\hbar = 1$ has been

used. The numerical values for the parameters are taken from Ref. 1. With our use of σ_2 instead of the conventional σ_3 , u and v correspond directly to amplitudes for even and odd sites of the chain, respectively.²⁰ On-site and nearest-neighbor electron correlations are described by

$$\mathcal{H}_U = U \sum_j n_{j\uparrow} n_{j\downarrow} \quad (3)$$

and

$$\mathcal{H}_V = V \sum_j n_j n_{j+1}, \quad (4)$$

where $n_{js} = c_{js}^\dagger c_{js}$ is the number of electrons with spin s on site j , c_n is the annihilation electron operator, and $n_j = n_{j\uparrow} + n_{j\downarrow}$. The inclusion of off-diagonal terms has been restricted in our calculations to the bond-charge repulsion term

$$\mathcal{H}_W = W \sum_l (B_{l,l+1})^2 \quad (5)$$

where $B_{l,l+1} = \sum_s (c_{ls}^\dagger c_{l+1,s} + c_{l+1,s}^\dagger c_{ls})$. We have ignored other usually considered "mixed" term involving both on-site and bond-charge effects, primarily because W appears to play a more relevant role than the mixed term.⁴ However, the main conclusions of this paper will be based primarily on on-site and nearest-neighbor interactions. The W term will only introduce minor corrections.

Consider the generalized Hartree-Fock wave function for the valence band $|\mathcal{V}\rangle = \prod_l c_{l\uparrow}^\dagger c_{l\downarrow}^\dagger |0\rangle$, where l and m refer to the continuum states. The total state containing n polarons or solitons can be represented simply as $|\Phi\rangle = \prod_\alpha c_{\alpha\uparrow}^\dagger c_{\beta\downarrow}^\dagger |\mathcal{V}\rangle$, where α and β refer to the bound states inside the gap. The expectation value of Eq. (1) with respect to $|\Phi\rangle$, according to the atomic orbital representation used in obtaining (2), is given by

$$\begin{aligned} \langle \mathcal{H}_{\text{TLM}} \rangle = & \frac{1}{2\pi\lambda v_f} \int dx \Delta(x)^2 \\ & + \sum_{k,s} n_{k,s} \int dx \Psi^\dagger [-iv_f \sigma_2 \partial_x + \Delta(x) \sigma_1] \Psi, \end{aligned} \quad (6)$$

$$\langle \mathcal{H}_U \rangle = Ua \int dx [Z_{10} Z_{10} + Z_{13} Z_{13}], \quad (7)$$

$$\begin{aligned} \langle \mathcal{H}_V \rangle = Va \int dx \sum_s [Z_{s0} (Z_{s0} + \mathcal{S}_{s0}) - Z_{s1}^2 - Z_{s2}^2 \\ - Z_{s3} (Z_{s3} + Z_{s3})], \end{aligned} \quad (8)$$

$$\begin{aligned} \langle \mathcal{H}_W \rangle = 2Wa \int dx \sum_s [-Z_{s0}^2 + Z_{s1}^2 + Z_{s3}^2 \\ + Z_{s2} (Z_{s2} + 2Z_{s2})] + 2WN, \end{aligned} \quad (9)$$

where $Z_{si} = \sum_k n_{k,s} \Psi_k^\dagger \sigma_i \Psi_k$, with σ_0 the identity matrix, $n_{k,s}$ the occupation number for state (k,s) , N the total number of electrons in the chain, and a the intersite distance.

For the amplitudes on the odd and even sites we have chosen the ones that satisfy the eigenvalue equation for the TLM Hamiltonian:

$$\begin{aligned} -v_f \partial_x v_k(x) + \Delta(x) v_k(x) &= \epsilon_k u_k(x), \\ v_f \partial_x u_k(x) + \Delta(x) u_k(x) &= \epsilon_k v_k(x). \end{aligned} \quad (10)$$

The energies $\epsilon_k = \pm \sqrt{\Delta_0^2 + k^2 v_f^2}$ refer to the conduction- and valence-band states. Electrons added to the system will occupy states which lie in the midgap region. Electron-hole symmetry guarantees that each electron added will produce two states symmetrically located with respect to $\epsilon=0$. These discrete states also satisfy (10), but with their respective energies $\omega_n = \pm \sqrt{\Delta_0^2 - k_n^2 v_f^2}$. For all cases, u and v satisfy the normalization constraint

$$\int dx [|u|^2 + |v|^2] = 1. \quad (11)$$

The expectation value of \mathcal{H}_{TLM} can now be written as

$$E_{\text{TLM}} = \frac{1}{2\pi\lambda v_f} \int dx \Delta(x)^2 + \sum_{k,s} n_{k,s} \epsilon_k. \quad (12)$$

The sum has to be carried out over continuum as well as discrete states of the chain. For a chain of length L , periodic boundary conditions²³ are imposed such that $kL = 2m\pi + \phi_k$, where $\phi_k = \sum_i^2 \tan^{-1} k/k_i$ for n excitations in the chain. In order to calculate Eq. (12) for the n -excitation state, we need the order parameter $\Delta(x)$. The following development leads to the solution. Equation (10) can be decoupled straightforwardly as

$$\begin{aligned} -\partial_x^2 v_n(x) + U_o(x) v_n(x) &= \lambda_n v_n(x), \\ -\partial_x^2 u_n(x) + U_e(x) u_n(x) &= \lambda_n u_n(x), \end{aligned} \quad (13)$$

where

$$\begin{aligned} U_o &= \frac{1}{v_f} \frac{\partial \Delta(x)}{\partial x} + \frac{1}{v_f^2} [\Delta(x)^2 - \Delta_o^2], \\ U_e &= \frac{-1}{v_f} \frac{\partial \Delta(x)}{\partial x} + \frac{1}{v_f^2} [\Delta(x)^2 - \Delta_o^2], \end{aligned} \quad (14)$$

the parameter $\lambda_n = 1/v_f^2 [\omega_n^2 - \Delta_o^2]$, and e and o stand for even and odd, respectively. These one-dimensional Schrödinger equations can be solved by the inverse scattering technique.^{24,25} In this account, the $U_{o,e}$ are determined in terms of the set of λ_n defined in Eq. (13). Then we can proceed to find the minimum of E_{TLM} by

$$\frac{\partial E_{\text{TLM}}}{\partial \omega} = 0, \quad (15)$$

where $\omega = \{\omega_1, \dots, \omega_n\}$. The minimizing set of $\{\omega_i\}_{\min}$ will be used to calculate the minimum energy of the stable configuration of electronic excitations. The order parameter is given then by inverting Eq. (14):

$$\begin{aligned} \frac{\partial \Delta(x)}{\partial x} &= \frac{v_f}{2} (U_o - U_e), \\ \Delta(x)^2 &= \Delta_o^2 + \frac{v_f^2}{2} (U_o + U_e). \end{aligned} \quad (16)$$

For very long chains, the inverse scattering theory yields²⁴

$$U_{o,e} = -2 \frac{d^2}{dx^2} \ln \det(A + I) \quad (17)$$

where $A_{m,n}^{e,o} = e^{\alpha_{e,o}^m} e^{\alpha_{e,o}^n} (e^{(k_n + k_m)x} / k_n + k_m)$. A relation between the set of $\{\alpha_{o,e}^n\}$ and the set of $\{\omega_i\}$ will be developed in the Appendix. Once this is achieved, $\{\omega_i\}$ will be the only undetermined set of parameters which are subsequently fixed by applying Eq. (15). The determinant in Eq. (17) has been evaluated explicitly for the n -excitation case. The expression is given in the Appendix, where we have defined $W_{o,e} \equiv \det(A + I)$.

With the order parameter in hand, we can now solve explicitly for E_{TLM} . We are particularly interested in the creation energies for excitations introduced into the gap. Let E_{TLM}^o be the energy of a uniformly dimerized undoped chain. The creation energy for an arbitrary number of excitations in the gap is

$$\delta E = \frac{4v_f \rho}{\pi} + \frac{4}{\pi} \sum_i \omega_i \tan^{-1} \frac{\omega_i}{k_i v_f} + \sum_i (n_+^i - n_-^i) \omega_i, \quad (18)$$

where $\delta E \equiv E_{\text{TLM}} - E_{\text{TLM}}^o$, $\rho = \sum_i k_i$, and $k_i v_f = \sqrt{\Delta_o^2 - \omega_i^2}$ where ω_i 's are the energies of the levels in the gap. The notation n_{\pm}^i denotes the occupation number for the negative and positive i th level in the gap. The energy E_{TLM}^o is calculated from Eq. (12) using $\Delta(x) = \Delta_o$ and carrying out the summation over k with the corresponding boundary condition $kL = 2m\pi$. In this way the quantity in Eq. (18) is the creation energy for the excitations introduced in the gap.

In order to calculate the energy of the full interacting Hamiltonian (1), we now have to determine the amplitudes u_n and v_n that describe the bound states in the midgap region. To this end, we must solve the eigenvalue equations (10) for the bound-state energies instead of the continuum energies ϵ_k . In analogy to inverse scattering for reflectionless potentials,²⁵ the wave functions of the bound states in the gap are given by

$$u_m(x) = e^{-k_m x} \left[1 - \sum_n \frac{2k_n e^{2\alpha_e^n} u_n(x) e^{-k_n x}}{k_n + k_m} \right], \quad (19)$$

where $v_m(x) = \text{sgn}(\omega_m) (-1)^{m+1} u_m(-x)$. The distorted valence- and conduction-band states are given by

$$u_k(x) = e^{ikx} \left[1 - \sum_n \frac{2k_n e^{2\alpha_e^n} u_n(x) e^{-k_n x}}{k_n - ik} \right]. \quad (20)$$

A useful approximation that much facilitates calculations is given by inserting (20) in the second equation of (10), and considering that the wave functions are slowly varying functions of the distance. In this limit

$$u_k(x) \cong \text{sgn} \epsilon_k \frac{ikv_f + \Delta(x)}{|\epsilon_k|} u_k(x). \quad (21)$$

The above expressions define the amplitudes for the wave functions up to a normalization factor that is subsequently determined by applying Eq. (11). The amplitudes of the wave functions in the continuum as well as those in the gap are now determined solely by solving the system given by (19). Details of the calculation, and explicit ex-

pressions for u_n in the n -excitation case, are given in the Appendix.

Thus far we have provided a means for calculating variationally the interacting creation energies of the n -excitation system for infinite chains. To consider finite chains, we proceed as follows. The condition for the vanishing of the potentials $U_{e,o}$ at the boundaries of the system imply that $\lim_{x \rightarrow \pm\infty} \Delta(x) = \pm\Delta_o$, as can be checked by Eq. (14). This means physically that at and near the boundaries, the system returns to the alternating bond configuration corresponding to uniformly dimerized chain. In order then to be able to consider smaller chain lengths and still be able to use inverse scattering theory we only need to impose $\lim_{x \rightarrow \pm L/2} \Delta(x) = \pm\Delta_o$, which is exactly the same condition except that now L enters explicitly in the calculation of the order parameter. Imposing this boundary condition on the second equation of (16), and using the fact that $U_{o,e} = -2(d^2/dx^2)\ln W_{o,e}$, we obtain

$$\Delta(x)^2 - \Delta_o^2 = G(x) + D(L), \quad (22)$$

where $G(x) = -v_f^2(d^2/dx^2)\ln(W_o W_e)$. The quantity $D(L)$, has to satisfy the conditions $D(L) = -G(\pm L/2)$ and $\lim_{L \rightarrow \pm\infty} D(L) = 0$. The first condition defines D and the second condition follows directly from the properties of $W_{o,e}$ as outlined in the Appendix. Now, applying the boundary condition on the first equation of (16), we obtain the relation

$$\Delta(x) = \frac{v_f}{2} \int dx (U_o - U_e) = f(x) + C(L), \quad (23)$$

where $f(x) = -v_f[W_o'/W_o - W_e'/W_e]$. Again, from the boundary conditions it follows that $C(L) = \Delta_o - f(\pm L/2)$. A relation can be found between D and C using the above equations, namely $D(L) = C(L)^2 - \Delta_o^2$.

Because our objective in this paper is to determine to what extent polarons are stable given their intrinsic attractive long-range interactions, we concern ourselves with an even number of extra electrons in the chain. Also, for simplicity we consider only even-number chains. Thus having even numbers of excitations and sites in a chain restrict further the boundary condition to $\Delta(\pm L/2) = \Delta_o$. Incorporating the modifications to the order parameter given by Eqs. (22) and (23) into Eq. (12), for the energy of the noninteracting part of the full Hamiltonian we obtain

$$\begin{aligned} \delta E = & \frac{-v_f}{\pi\lambda} \left[\frac{W_o' \left(\frac{L}{2} \right)}{W_o \left(\frac{L}{2} \right)} + \frac{W_e' \left(\frac{L}{2} \right)}{W_e \left(\frac{L}{2} \right)} \right] \\ & + \frac{L}{2\pi\lambda v_f} (C^2 - \Delta_o^2) + \frac{2v_f}{\pi} \left[2 + \frac{1}{\lambda} \right] \sum_i k_i \\ & + \frac{4}{\pi} \sum_i \omega_i \tan^{-1} \frac{\omega_i}{k_i v_f} + \sum_i (n_+^i - n_-^i) \omega_i. \quad (24) \end{aligned}$$

Note that from the limiting properties of $W_{o,e}$, as outlined and shown in the Appendix, $\lim_{L \rightarrow \infty} ([W_o'(L/2)/W_o(L/2)] + [W_e'(L/2)/W_e(L/2)]) = 2\sum_i k_i$, Eq. (18), as expected. The energy of the full Hamiltonian (1) as a function of the length of the chain can now be calculated by inserting the wave functions described above into Eqs. (7)–(9), and adding the contribution from the noninteracting part as given by (24). The configuration of the energy levels that render the energy a minimum will be given by Eq. (15) using the total interacting energy instead of E_{TLM} . The nature of the final state, either a polaron or soliton state, will be determined by the lowest energy of the two configurations.

A comment on Eq. (22) is in order. Because the inverse scattering formalism requires that $U_{o,e}(L/2) \rightarrow 0$ then the vanishing of the potential at the boundaries is true as long as $\Delta(x) \rightarrow \Delta_o$ and $\partial\Delta(x)/\partial x \rightarrow 0$ at $x = L/2$. By adding parameter $D(L)$ in Eq. (22), we are effectively adding parameter D/v_f^2 to the potentials $U_{o,e}$, as can be checked by direct substitution of Eq. (22) into Eq. (14). This means that the parameter D has to be a small number. Because $D(L)$ is a decreasing function of the length of the chain L , in order to maintain D small, L cannot be taken to be arbitrarily small. As a consequence of this, our calculations cannot be applied to arbitrarily high concentrations (small L). A criterion that gives good numerical results is that minimum value of L should not be smaller than the combined widths of the excitations in the chain. That is, if there are n polarons of width d each in a chain, L should satisfy $L \geq nd$.

III. RESULTS

Because of the complexity of the expressions for the functions $W_{o,e}$ and the wave functions for both continuum and bound states, the minimization calculations as well as the calculations for the energy were carried out numerically. In the doping process, each added electron will introduce a new bound-state energy parameter ω_i . This means that for n added electrons there will be an n -dimensional set of ω_i 's on which the energy must be minimized. Such a multidimensional minimization is far from straightforward numerically. We have chosen to use algorithms that make use of the derivatives of the function to be minimized. Though time consuming, this procedure exceeds the efficiency of convergence reached by interpolation methods. Also, because we are concerned with doping of two electrons at a time for each chain, the computational time for the minimizations in each subsequent doping step more than doubles. Results will be presented for two, four, and six electrons added to a chain. For comparison purposes, all results will be presented in terms of the concentration n/N , where N is the number of sites in the chain. We will only consider in the doping process the addition of extra electrons to the chain. Electron-hole symmetry guarantees that hole doping will yield identical results. As is well known, the occupations of the soliton and polaron states differ. This fact will prove to be relevant because the interactions will contribute in each case according to their occupations. For negative doping, the polaron state possesses a half-

filled uppermost state, while the soliton state has a doubly filled state.

For comparison purposes we define $\Delta E \equiv E_p - E_s$, where E_p and E_s are the corresponding interacting creation energies for a polaron and soliton configurations, as described at the end of Sec. II. The point at which $\Delta E=0$ marks the transition from one to the other configuration. In Fig. 1 we present ΔE a function of U for the cases of two, four, and six extra electrons in an $N=200$ chain. It is calculated for the case of $V=W=0$. The value for U at which $\Delta E=0$ indicates a point beyond which a polaron state has lower creation energy than a soliton one. We call this critical value for U , U_c . The fact that the soliton state reaches a point at which its creation energy surpasses that of the corresponding polaron state can be understood in the sense that an on-site repulsion term will be most costly for those configurations containing double occupancy of the same site, or in our case to the same state. Thus after the interaction strength increases beyond U_c the polaron configuration of singly occupied states has a lower total energy than the doubly occupied one for the solitons. An alternative way of thinking about these results is that electron-electron repulsions are needed in order to stabilize a polaron lattice, because the interaction between polarons is intrinsically attractive and long range. One point to note is that U_c increases as the number of added electrons increases. This is the same as saying that for increasing concentration (from 1% to 3%) the on-site repulsion needed to drive a transition increases. One might expect the contrary by noting that the slope of ΔE for greater numbers of electrons seems to increase. The crucial relationship, however, is that the value of ΔE at $U=0$ increases much faster as the doping increases.

The values of U_c can be collected and plotted as a function of decreasing N , as in Fig. 2, where the x axis is n/N ($=\%$). Nearest-neighbor interactions have been included in this figure for values of $V=0.2$ and 0.4 eV. The results presented are only for the case of two elec-

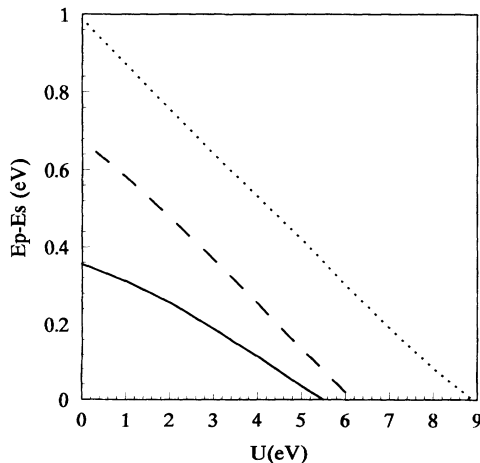


FIG. 1. ΔE as a function of on-site repulsion U for two (solid), four (dashed), and six (dotted) electrons in a chain of $N=200$ ($V=W=0$).

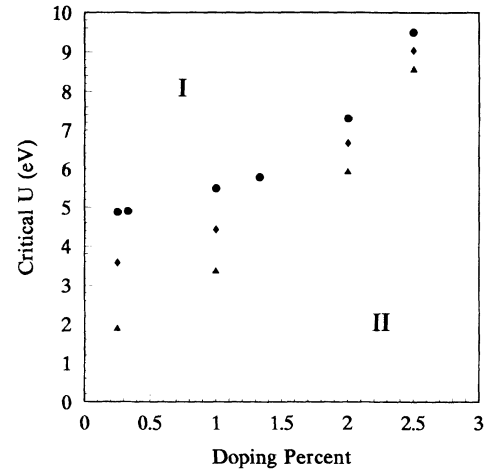


FIG. 2. Critical on-site repulsion U_c vs concentration for two electrons in the chain. The results presented are for $V=W=0$ (circles), $V=0.2$, $W=0$ (diamonds), and $V=0.4$, $W=0$ (triangles). Phases I and II stand for stable regions of polarons and solitons, respectively.

trons in the chain, but the general trend is true for any amount of doping. The upper region marked I and the one marked II correspond to regions where polarons and solitons are favored, respectively. The trend of increasing U_c as a function of concentration is clear, demonstrating that given some value of U at 0% in phase II the soliton phase will persist. If one were to start in phase I, however, there would be a concentration beyond which solitons would be favored. The result that V shifts the curves downward, therefore favoring polarons, can be explained in terms of charge distributions. Because the charge distribution for a soliton is more localized than in polarons, and is only distributed in either even or odd sites, an overlapping soliton-antisoliton pair will gain more interaction energy from the V term than the corresponding polaron system. Thus V as well as U favors the polaron systems as a function of their strength.

In Fig. 3 we have considered the case of $V=W=0$ for two, four, and six electrons in the chain. The pattern shown in Fig. 3 as the number of electrons is increased suggests that there is a limiting boundary for large n and N (but fixed n/N). We have extrapolated this behavior and presented a limiting curve as a dashed line. The limiting curve seems to exhibit the same behavior as do the others. This means that increasing concentration will not yield a polaron phase had we started in the soliton phase. We conclude then that it is unlikely that on-site repulsion is responsible for the metal transition as a function of its strength, although it *does* yield a transition as a function of its strength. Also from Fig. 2 we see that, for increasing nearest-neighbor repulsion V , a smaller U_c can be achieved. However, nearest-neighbor repulsions ultimately stabilize the soliton phase once the doping is considered.

The nondiagonal term W has been considered in Fig. 4, where we present a phase diagram of W_c vs V at a value of $U=4$ eV for $N=200$. The values for W_c have been

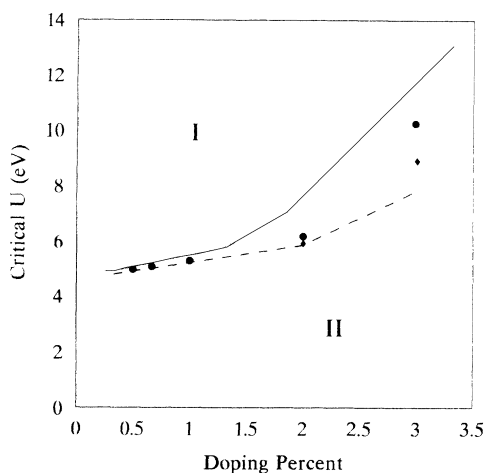


FIG. 3. Critical on-site repulsion U_c vs concentration for $V=W=0$. The solid line corresponds to two, circles to four, and diamonds to six electrons. The dashed line represents an extrapolation to a system with an infinite number of doped electrons.

calculated in the same way as was done for the values of U_c . At a fixed value of U and V , the value of W at which $\Delta E=0$ is W_c . The bond-charge W term is seen to have a different behavior from the other two terms. As a function of its strength the system, if in phase I, is driven into phase II; that is, it breaks the polaron state into a soliton phase. On the other hand, W follows the same behavior as a function of the number of electrons in the chain, as do V and U . That is, it moves the boundary toward higher V , thereby destabilizing the polaron phase as a function of doping.

Some general statements can be made regarding the closure of the gap, based on the behavior of the bound state levels as a function of doping. By examining the set of $\{\omega_i\}$ that minimizes the energy for the noninteracting as well as the interacting cases, the expected general

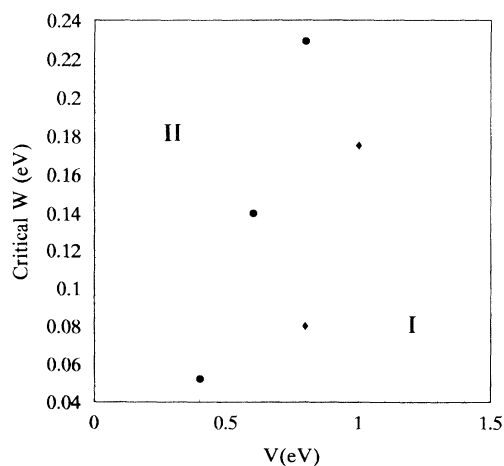


FIG. 4. Critical value of W vs V at $U=4$ for $N=200$. Circles correspond to two (1%), and diamonds to four electrons (2%).

trend that the levels start to form bands is observed. There are bands in the middle of the gap and at the symmetrically located levels for the soliton and polaron configurations, respectively. Up to the doping levels achieved in this paper (around 3%) the levels seem to reduce the gap down to a value of the order of 0.3 eV. The widening of the bands as a function of doping seems to obey a power law. Future work will consider relevant physical quantities (e.g., the magnetic susceptibility) making use of a more detailed analysis of the rate of closure of the gap as a function of doping.

In conclusion, we have shown how a transition from solitons to polarons in *trans*-polyacetylene can be achieved as a function of U alone, or U and V . W seems to break or dissociate polarons into solitons. This is related to other findings at half-filling, in which W increases dimerization.¹⁸ In all the cases shown above an increase in concentration, via the decrease of the length of the chain or by increasing the number of electrons in the chain, ultimately favors solitons up to the concentration of 3%. However, we have no reason to believe that this trend will not continue to doping levels beyond 3% and into the metallic regime. We are then faced with the original question: what drives the onset of spins in polyacetylene? It has been proposed by several authors that interchain coupling effects must be included to describe the onset of the metal state in polyacetylene. Current estimates of the interchain hopping matrix element are around 0.15 eV.¹⁴ Based on our calculations, we can now estimate if an effect of this magnitude is sufficient to destabilize the soliton lattice at 5%. At a doping level of 5%, where $U=4$ eV, and $V=0.4$ eV, we estimate that a soliton lattice is more stable than the corresponding polaron one by 0.6 eV. Interchain coupling effects of 0.6 eV or higher would certainly then be sufficient to break up solitons on single chains. However, based on the estimates in the literature of t_{\perp} , it is unlikely if such effects are ultimately responsible for the transition from a soliton to a polaron lattice in *trans*-polyacetylene at the metal-insulator transition. Further calculations which include short-range electron corrections are clearly necessary to settle the precise role of interchain coupling on the insulator-metal transition in polyacetylene.

ACKNOWLEDGMENTS

We are grateful to Qiming Li for stimulating and helpful discussions. This work was supported by the National Science Foundation through Grant No. DMR 90-22933.

APPENDIX

Before deriving the exact expression for the wave functions, we define some of the notation to be used in this Appendix. We will define objects with an arrow overhead to indicate the vector form of that set, e.g., $\mathbf{k}=(k_1, k_2, \dots)$ and $\boldsymbol{\delta}=(\delta_1, \delta_2, \dots)$, whose dimension (number of elements) is given by the number s of levels (electrons) introduced into the gap. Subscripts on these objects indicate the same vector, but with the subscript

element omitted. For example, $\mathbf{k}_1 = (k_2, k_3, \dots)$, so that this new vector has dimension $s-1$. A matrix L of dimension $2^{s-1} \times s$ whose elements are either 1 or -1 will be used. Its row vectors L_{nm} will be denoted for convenience by two indices. The first index n denotes how many -1 elements it has, and the second m denotes which row vector it is. The definition of this L matrix is given below. By the dot product $L_{nm} \cdot \mathbf{k}$, for example, we denote the dot product of the specified L_{nm} row vector with \mathbf{k} . If a superscript is included such as $L_{nm}^1 \cdot \delta_s$, the dot product is carried between the δ vector, whose s ele-

ment has been omitted, with the L_{nm} row vector, whose element number 1 also has been omitted. A matrix P will be used, and it is constructed in the same way as the L matrix, but with dimension $2^{s-2} \times (s-1)$ instead. In both cases $P_{nm}(j)$ or $L_{nm}(j)$ refer to the element j of the row vector of the respective matrix. The rules for the construction of the L matrix, and so for the P matrix, are given below.

The wave functions that solve the system (19) were derived by induction, and are given for any number s of levels ($s > 1$) by

$$u_q = \frac{1}{W_e} \prod_{j>q}^s \sigma_{qj} \exp -1/2 \left[\sum_{i=1}^s \delta_{i-(s-2)\delta_s} \right] \sum_{n=0}^{s-2} \sum_{m=1}^{\binom{s-2}{n}} a_{nm}^{q-1} C_{nm}^q F_q \{ \beta_{nm}^q x - \frac{1}{2} (\delta_s \cdot P_{nm} + [2n+1-s]\delta_s) \} \quad (\text{A1})$$

for $q=1$, and

$$u_q = \frac{1}{W_e} \prod_{j<q}^{q-1} \sigma_{jq} \prod_{j>q}^s \sigma_{qj} e^{-1/2(\delta_{q-1}-\delta_s)} \sum_{n=0}^{s-2} \sum_{m=1}^{\binom{s-2}{n}} a_{nm}^{q-1} C_{nm}^q F_q [\beta_{nm}^q x - \frac{1}{2} \gamma_{nm}^{sq}] \quad (\text{A2})$$

for $q > 1$, where $F_q[] \equiv \sinh[]$, or $\cosh[]$ for q even or odd, respectively. Also $\beta_{nm}^q \equiv \mathbf{k}_q \cdot P_{nm}$, $\sigma_{ij} = k_i - k_j$ and

$$\gamma_{nm}^{sq} \equiv \alpha_{nm}^s + \sum_{j=2}^{q-1} a_{nm}^j a_{nm}^{j-1} (\delta_{j-1} - \delta_j), \quad (\text{A3})$$

$$\alpha_{nm}^s \equiv \delta_s \cdot P_{nm} + \sum_{i=2}^{s-2} \delta_i + [2(n-s)+5]\delta_s. \quad (\text{A4})$$

Other symbols used above are defined as follows:

$$C_{nm}^q \equiv \prod_{n < v \neq q}^s \{ k_\eta - k_v [P_{nm}(\eta - \delta_{\eta>s}) P_{nm}(v - \delta_{v>s})] \} \quad (\text{A5})$$

and

$$a_{nm}^q = \prod_{j=1}^q P_{nm}(j), \quad (\text{A6})$$

where $a_{nm}^0 = a_{nm}^{-1} = 1$ and $\delta_{i>j} \equiv \theta(i-j)$ is the normal step function. Note that wave functions (A1) and (A2) are given in terms of a set $\{\delta\}$ instead of the set $\{\alpha\}$ introduced in Eq. (19). The transformation was done for convenience, and is given by

$$e^{2\alpha_e^1} = \prod_{j=2}^s \frac{\rho_{1j}}{\sigma_{1j}} \exp \left[\sum_{i=1}^s \delta_i - (s-2)\delta_s \right] \quad (\text{A7})$$

for $q=1$, and

$$e^{2\alpha_e^q} = \prod_{j=2}^{q-1} \frac{\rho_{jq}}{\sigma_{jq}} \prod_{j=q+1}^s \frac{\rho_{qj}}{\sigma_{qj}} e^{(\delta_{q-1}-\delta_s)} \quad (\text{A8})$$

for $q > 1$, where $\rho_{i,j} = k_i + k_j$. The term W_e in the denominator of u_q , which is the determinant of the ma-

trix $(A+I)$, as defined in the paragraph containing Eq. (17),

$$W_e(x) = \sum_{n=0}^{s-1} \sum_{m=1}^{\binom{s-1}{n}} D_{nm}^s \cosh \left[(L_{nm} \cdot \mathbf{k})x - \frac{1}{2} L_{nm}^1 \cdot \delta_s - \frac{1}{2} \sum_{i=1}^{s-1} \delta_i - (n+2-s)\delta_s \right], \quad (\text{A9})$$

where we have used the short-hand notation

$$D_{nm}^s \equiv \prod_{i<j}^s \{ k_i - k_j [L_{nm}(i) L_{nm}(j)] \}. \quad (\text{A10})$$

Note that for $s=1$ the only wave function is $u_1 = e^{-\delta_1} / 2W_e$. The amplitude for the odd sites v_q can be obtained from the relation $v_q(x) = \text{sgn}(\omega_q) (-1)^{q+1} u_q(-x)$, and since it also satisfies a relation similar to Eq. (19),

$$v_q(x) = e^{-k_q x} \left[1 - \sum_n \frac{2k_n e^{2\alpha_n^q} v_n(x) e^{-k_n x}}{k_n + k_q} \right], \quad (\text{A11})$$

it can be shown that $W_e(x) = W_o(-x)$.

The L matrix is defined as follows. The first column of this matrix is composed of $+1$ elements only, and the rest of the matrix follows an ordering that exhausts all the combinations of $+1$ and -1 . The form used in this paper for a given s , n , and m is as follows. Let the indices i, j, k, \dots, l denote the individual L row-vector element positions whose values are equal to -1 , where $i < j < k < \dots < l$, and there are n of them. Then

$$\begin{aligned}
L_{nm}(i) &= -1 \quad \text{if} \quad \binom{s-i}{n} < m \leq \binom{s+1-i}{n}, \\
L_{nm}(j) &= -1 \quad \text{if} \quad \binom{s-i}{n-1} < m - \binom{s-i}{n} \leq \binom{s+1-j}{n-1}, \\
&\vdots \\
L_{nm}(k) &= -1 \quad \text{if} \quad \binom{s-k}{n-2} < m - \binom{s-i}{n} - \binom{s-j}{n-1} \leq \binom{s+1-k}{n-2}, \\
&\vdots \\
L_{nm}(l) &= -1 \quad \text{if} \quad \binom{s-l}{n-2} < m - \binom{s-i}{n} - \binom{s-j}{n-1} - \binom{s-k}{n-2} - \cdots - \binom{s-t}{2} \leq \binom{s+1-l}{1}.
\end{aligned} \tag{A12}$$

All other elements that do not satisfy these conditions are equal to +1. Note that for a given m and n the first line of Eq. (A12) completely determines the position of the first -1 in the row vector i . Once this position is determined, it is used in the second line to determine the next position j , and so on. The matrix P is constructed in exactly the same way as the L matrix, but using $s-1$ instead of s .

From Eqs. (A7) and (A8) we have a relation between the set of $\{\alpha_e^n\}$ and a set of $\{\delta_i\}$, which turns out to be convenient in our case. Now we present the relation between $\{\delta_i\}$ and $\{\omega_i\}$, therefore establishing the dependence of u_q on the energy levels. Let us define the quantity $Q_i \equiv k_i v_f / C(L)$, where $C(L) = \Delta_0 - f(L/2)$, as defined in the text following Eq. (23). Also defining the vector $\mathbf{R} = (R_1, R_2, \dots, R_s)$, where its individual elements are further defined by $R_i \equiv \tanh Q_i$, we have

$$\delta_s = \frac{1}{2} L_{(s-1),1} \cdot \mathbf{R} \tag{A13}$$

for $q=s$, and

$$\delta_q = \frac{1}{2} L_{(s-2),q} \cdot \mathbf{R} \tag{A14}$$

for $q < s$. Thus, starting from a given set of $\{\omega_i\}$, by Eqs. (A13) and (A14) we obtain the corresponding $\{\delta_i\}$. The values of $\{k_i\}$ are determined by $k_i v_f = \sqrt{\Delta_0^2 - \omega_i^2}$, so that all the values of σ_{ij} and ρ_{ij} are determined. In conclusion, by the above developments the wave functions (A1) and (A2) depend solely on the parameters $\{\omega_i\}$, the energy levels of the bound states.

Now we proceed to show how Eq. (18) can be obtained from Eq. (24). The sufficient relation comes from examining Eq. (A9) in the limit of $L \rightarrow \pm\infty$. Note that for very large x we obtain $W_e(x) \cong D_{01}^s \cosh[(L_{01} \cdot \mathbf{k})x]$, since the largest term in the sum is the one in which all values of $\{k_i\}$ are summed. For its derivative we then obtain $W_e'(x) \cong (L_{01} \cdot \mathbf{k}) D_{01}^s \cosh[(L_{01} \cdot \mathbf{k})x]$. Then the condition follows that $\lim_{L \rightarrow \pm\infty} [W_e'(x)/W_e(x)] = \sum_i k_i$. Thus Eq. (18) is obtained by considering that in this limit the quantity $C(L) - \Delta_0$ also vanishes.

¹W.-P. Su, J. R. Schrieffer, and A. J. Heeger, Phys. Rev. B **22**, 2099 (1980).

²D. K. Campbell, T. A. DeGrand, and S. Mazundar, Phys. Rev. Lett. **52**, 1717 (1984).

³J. E. Hirsch, Phys. Rev. Lett. **51**, 296 (1983).

⁴S. Kivelson, W.-P. Su, J. R. Schrieffer, and A. J. Heeger, Phys. Rev. Lett. **48**, 1899 (1987).

⁵W.-K. Wu and S. Kivelson, Phys. Rev. B **33**, 8546 (1986).

⁶J. E. Hirsch and M. Grabowski, Phys. Rev. Lett. **52**, 1713 (1984).

⁷K. A. Chao and S. Stafström, Mol. Cryst. Liq. Cryst. **118**, 45, (1985).

⁸D. K. Campbell, J. Tinka Gammel, and E. Y. Loh, Synth. Met. **27**, A9 (1988).

⁹F. Moraes, J. Chen, T.-C. Chung, and A. J. Heeger, Synth. Met. **11**, 271 (1985).

¹⁰S. Kivelson, and A. J. Heeger, Synth. Met. **17**, 183 (1987).

¹¹Y. H. Kim and A. J. Heeger, Phys. Rev. B **40**, 8393 (1989).

¹²E. M. Conwell, H. A. Mizes, and H.-Y. Choi, Synth. Met. **41-43**, 3675 (1991).

¹³S. Stafström, Phys. Rev. B **43**, 9158 (1991).

¹⁴H. A. Mizes and E. M. Conwell, Phys. Rev. Lett. **70**, 1505 (1993).

¹⁵S. A. Kivelson and M. I. Salkola, Synth. Met. **44**, 281 (1991).

¹⁶S. Stafström and K. A. Chao, Phys. Rev. B **30**, 2098 (1984).

¹⁷H. Takayama, Y. R. Lin-Liu, and K. Maki, Phys. Rev. B **21**, 2388 (1980).

¹⁸D. K. Campbell, J. Tinka Gammel, and E. Y. Loh, Phys. Rev. B **38**, 12 043 (1988).

¹⁹S. Okuno and Y. Onodera, J. Phys. Soc. Jpn. **52**, 3495 (1983).

²⁰Y. Onodera and S. Okuno, J. Phys. Soc. Jpn. **52**, 2478 (1983).

²¹M. Grabowski, D. Hone, and J. R. Schrieffer, Phys. Rev. B **31**, 7850 (1985).

²²Yu. N. Garstein, Synth. Met. **44**, 219 (1991).

²³S. Kivelson, T.-K. Lee, Y. R. Lin-Liu, I. Peschel, and L. Yu, Phys. Rev. B **25**, 4173 (1982).

²⁴I. Kay and H. E. Moses, J. Appl. Phys. **27**, 1503 (1956).

²⁵V. E. Zakharov and A. B. Shabat, Zh. Eksp. Teor. Fiz. **61**, 118 (1971) [Sov. Phys. JETP **34**, 62 (1972)].